Available online at www.sciencedirect.com
SCIENCE DIRECT®
ELSEVIER
Microelectronic Engineering 70 (2003) 109–114
MICROELECTRONIC ENGINEERING
www.elsevier.com/locate/mee

Wet etching studies of silicon nitride thin films deposited by electron cyclotron resonance (ECR) plasma enhanced chemical vapor deposition

K.B. Sundaram[a,*], R.E. Sah[b], H. Baumann[c], K. Balachandran[a], R.M. Todi[a]

[a]School of Electrical Engineering and Computer Science, University of Central Florida, Orlando, FL 32816-2450, USA
[b]Fraunhofer-Institut für Angewandte Festkörperphysik, Tullastrasse 72, D-79108 Freiburg, Germany
[c]Institut für Kernphysik, J.W. Goethe Universität, D-60486 Frankfurt, Germany

Received 29 May 2003; accepted 24 June 2003

Abstract

Silicon nitride films of various compositions have been deposited on silicon substrate by electron cyclotron resonance plasma-enhanced chemical vapor deposition (ECR-PECVD) technique from mixtures of Ar, N_2 and SiH_4 as precursors. Film composition and refractive index as a function of deposition parameters like gas flow ratio and pressure were studied. Wet etching studies were conducted using diluted phosphoric acid and buffered oxide etch (BOE) solutions of various concentrations. The etching studies using phosphoric acid were conducted in the temperature range of 70–90 °C. For BOE the temperature range was 25–55 °C. The etch rate with BOE solution is much higher than with phosphoric acid. The results indicate that the mechanism of etching with phosphoric acid is different from that with BOE solution.

Keywords: Silicon nitride films; Wet etching; ECR-PECVD

1. Introduction

Thin films of silicon nitride (SiN) are widely used as isolation, dielectric, passivation layers or optical coatings for various electronic and optoelectronic devices [1–3]. They are also used as gate dielectric in MOS devices [4,5]. They have found applications as diffusion masks and encapsulants for thermal annealing [6,7]. They are also increasingly used in microelectromechanical system (MEMS) device fabrication [8,9]. Recently for the copper dual damascene chemical mechanical polishing process, silicon nitride films are used as etch stop layers [10]. One of the techniques used for the deposition of the films is an ECR-PECVD technique [11], which is a high-density plasma deposition technique. This technique provides low ion-energy bombardment and low plasma damage [12]. In addition, the technique allows the deposition of SiN films at low deposition temperatures with a low amount of hydrogen [13]. Yota et al. [14] showed that high density plasma CVD (HDP CVD) silicon nitride film has a higher film density, much lower hydrogen content, in addition to lower polish, wet-etch and dry-etch rates, than the PECVD film. It has also been reported that ECR-PECVD deposited films have superior water

*Corresponding author. Tel.: +1-407-823-5326; fax: +1-407-823-5835.
E-mail address: sundaram@mail.ucf.edu (K.B. Sundaram).

0167-9317/03/$ – see front matter
doi:10.1016/S0167-9317(03)00412-X

blocking ability to conventional parallel-plate PECVD deposited films [15]. Etching of silicon nitride is very important in many applications and device processing. The etching can be accomplished either by dry etching or wet etching process. Dry etching of SiN films has been studied extensively by several authors [16–19]. Though dry etching has several advantages over wet etching, some applications require SiN films to be etched by wet etching process. Examples include sacrificial layers in micromachining and selective etching in localized oxidation of silicon dioxide (LOCOS). Wet etching of conventional SiN films has been studied by several authors using buffered oxide etch (BOE) and HF solutions [20–25]. Some results on etching of ECR-plasma deposited SiN films using BOE have been reported by Buckle et al. [26]. A detailed study is still lacking. Wet etching process using phosphoric acid may be necessary in applications where selective etching of SiN is needed in presence of silicon dioxide as mask layers.

In the present work, we report the results of detailed studies on the wet etching of SiN films deposited using ECR-PECVD technique. The etching studies were performed at different temperatures using phosphoric acid and BOE as a function of important deposition parameters.

2. Experimental

The SiN films of various compositions were deposited from mixtures of Ar, N_2 and SiH_4 as precursors on ⟨100⟩ silicon substrates using a PlasmaTherm ECR-PECVD system (SLR 770). The system was equipped with an Astex® AX4400 ECR plasma source and a load lock. The base pressure was 1.2×10^{-7} Torr. The mixture of Ar and N_2 was introduced in the ECR source, while undiluted SiH_4 was introduced downstream through a gas dispersal ring near the substrate in the deposition chamber. The total flow rate of precursor gases, V, and the deposition temperature, T_S, were kept constant at 55 sccm and 90 °C, respectively, for all depositions. The deposition pressure P was varied from 1.5 to 55 mT.

The film thickness and refractive index were determined by measuring ellipsometric parameters Ψ and Δ with a Woolam variable angle spectroscopic ellipsometer in the spectral range 0.8–5.0 eV and evaluating the measurements using Cauchy's dispersion relation [11]. The deposition rate was calculated using the measured film thickness and deposition time. In the present study, the SiN films were between 110 and 170 nm thick.

The determination of H content in the film is based on the nuclear reaction $^{15}N(^1H,\alpha,\gamma)^{12}C$ analysis [27]. A 7-MeV Van de Graaf accelerator has been used for the nuclear reaction. The nuclear reaction has a narrow resonance in the excitation function at 6.385 MeV. The γ-rays from the nuclear reaction were measured with two 8×4″ NaI detectors. An ammonium chloride sample was used as a standard to determine the absolute H content in the films.

The determination of elements other than H in the films was performed using RBS with the (α,α) resonant backscattering reactions [28,29] at the energy of the probing ^4He ion beam of 3.5 MeV. The elastically backscattered particles were detected by a silicon surface barrier detector at an angle of 171° relative to the incident ion beam. To enhance the depth resolution, the samples were tilted to an angle of 75° with respect to the analyzing beam direction. The relative concentrations of Si, N, and Ar in the films were determined by comparing experimental and simulated backscattering spectra using the computer program RUMP [28]. No oxygen signal was observed in the spectrum within the detection limit (5 at%) of our RBS measurements.

Wet etching studies were performed using two etchants, namely phosphoric acid (85% H_3PO_4) and buffered oxide etch (BOE) solution. BOE consisted of 9 parts of NH_4F (40%) and 1 part of HF (49%) by volume. For some experiments both etchants were further diluted with water shortly before they were used. A temperature-controlled bath was used to study the etching behavior at different temperatures. During the course of etching the color of the SiN film was continuously monitored and the final completion of etching was determined by the hydrophobic behavior of silicon. The etch bath was covered with a glass lid to prevent any appreciable loss of water due to evaporation. The etching rates for various conditions were determined by repeating the experiment under identical conditions for at least four to five samples.

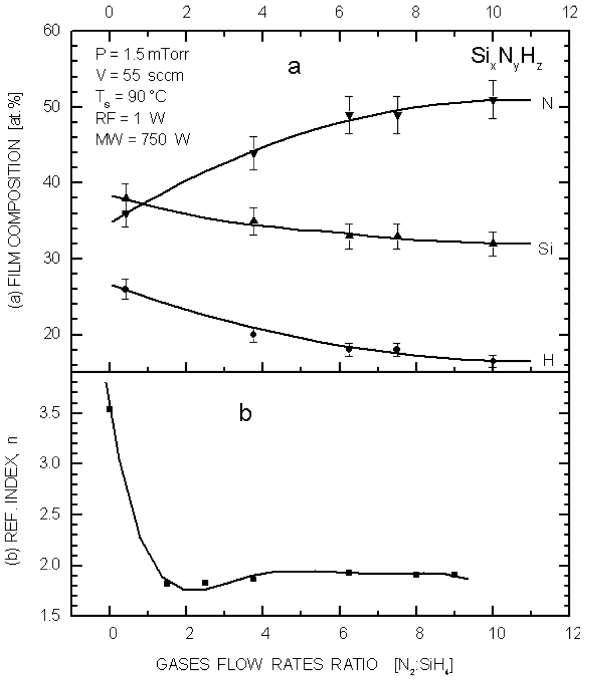

Fig. 1. Dependence on flow rate ratio N_2:SiH_4 of (a) the composition and (b) the refractive index (λ=1000 nm) of SiN films.

3. Results and discussions

3.1. Film composition

Fig. 1 shows the variation of the composition and refractive index at a wavelength λ=1000 nm of SiN films with the gases flow rates ratio, N_2:SiH_4, for a given V=55 sccm at P=1.5 mTorr. The gas flow rate ratio, N_2:SiH_4, was varied by varying the flow rates of N_2 and Ar while keeping the flow rate of SiH_4 and the total flow rate of Ar, N_2 and SiH_4 constant. In the given range of flow rate ratios the amount of Si and that of H in the films decreases, while that of N increases with increasing flow rate ratio N_2:SiH_4 (Fig. 1a). These results are consistent with the idea that the higher the flow rate of N_2, the higher the amount of incorporated N in the films. The refractive index, n, of the film dropped from 3.57 to 1.77 (Fig. 1b) in the range of N_2:SiH_4=0–2, the highest n being for the amorphous silicon film deposited from the mixture of Ar and SiH_4 with the flow rates ratio Ar:SiH_4=51:4. At higher N_2:SiH_4, in the range of 2–7, the concentration of N in the films increased from 40 to 49 at%, while that of H decreased from 22 to 17 at%, the amount of Si remaining almost unchanged.

Fig. 2 shows the variation of the composition and the refractive index of the films as a function of pressure P for a given flow ratio, N_2:SiH_4. In this case the amount of Si and that of H in the films increases, while that of N decreases (Fig. 2a) in the given range of P. The refractive index of the film (λ=1000 nm) increased (Fig. 2b) in the P range of 7–55 mTorr due, in this case, to an increase in the Si content of the film.

3.2. Etching with phosphoric acid

Figs. 3 and 4 show the dependence of the etch rate with phosphoric acid on the deposition parameters P and flow rate ratio of precursors (N_2:SiH_4) at different etching temperatures as marked in figure.

Up to 40 mT (Fig. 3) the deposition pressure, P, has relatively weak influence on the etch rate. The etch rate increases only slightly up to this pressure. At higher P it increases sharply. Furthermore, it can also be noticed that the etch rate increases strongly with etching temperature. Initially the hydrogen

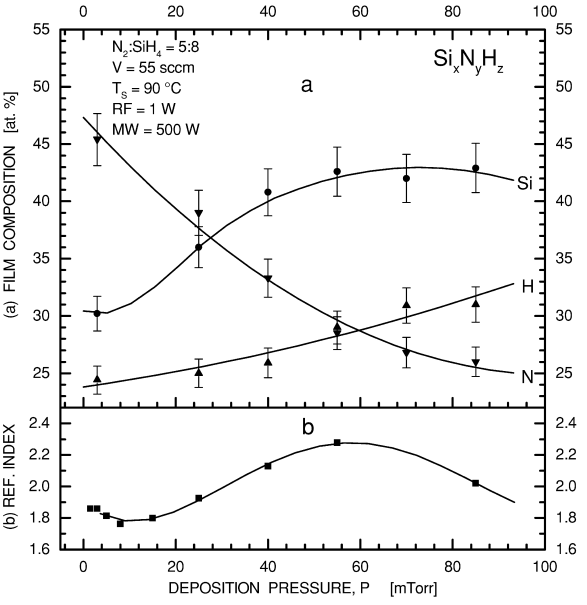

Fig. 2. Dependence on deposition pressure of (a) the composition and (b) the refractive index (λ=1000 nm) of SiN films.

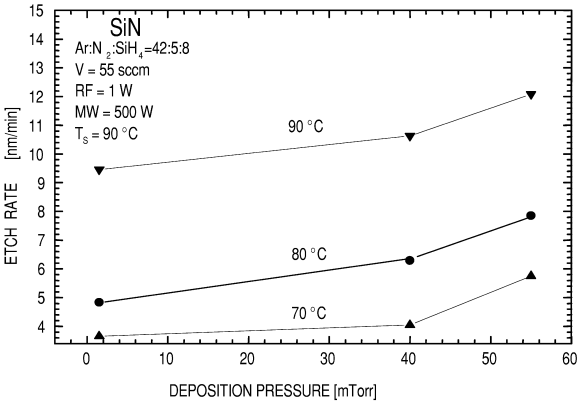

Fig. 3. Etch rate with undiluted phosphoric acid at 70, 80, and 90 °C as a function of deposition pressure.

composition in the film is low and nitrogen composition is high (Fig. 2) resulting in a fairly low etch rate up to a pressure of 40 mT. Gradually the hydrogen content increases which results in a higher etch rate. It is also observed that the silicon composition remains fairly constant beyond the deposition pressure of 40 mT.

The flow rate ratio N_2:SiH_4 (Fig. 4) has a strong influence on etch rate. The dependence passes through a minimum. With N_2:SiH_4<5.5 the etch rate decreases while with N_2:SiH_4>5.5 it increases. The minimum value of the etch rate is around 4 nm/min for N_2:SiH_4~5.5 and for the combination of other deposition parameters given in the figure. The dependence is similar at all etching temperatures studied.

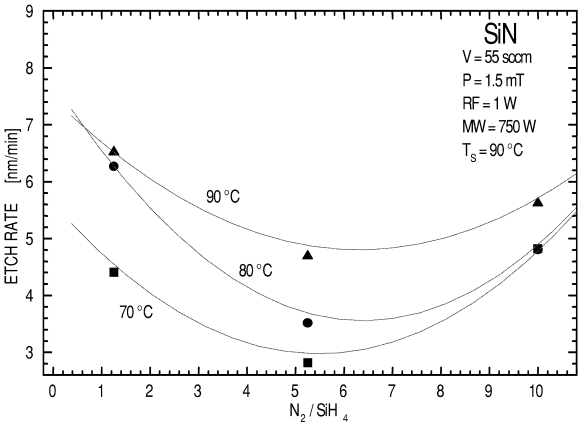

Fig. 4. Etch rate with undiluted phosphoric acid as a function of flow rate ratio of precursors.

At low ratios of N_2:SiH_4 the film has more hydrogen content (Fig. 2) leading to a higher etch rate. At higher ratios the increase in nitrogen is more dominant than the decrease in hydrogen and also the silicon decreases very gradually. A combination of all these effects leads to a minimum etching rate at ratio of ~5.5 followed by an increase beyond this ratio.

Fig. 5 shows the dependence of the etch rate on concentration of phosphoric acid in water at different etching temperatures. The basic chemical reaction for silicon nitride etch in phosphoric acid can be modeled by the hydrolysis process:

$$3Si_3N_4 + 27H_2O + 4H_3PO_4 \Leftrightarrow 4(NH_4)_3PO_4 + 9H_2SiO_3 \quad (1)$$

Eq. (1) suggests that water is hydrolyzing the silicon nitride to form hydrous silica and ammonia, the ammonia remains in the solution in the form of ammonium phosphate. Hence water is an integral part of the reaction mechanism. Here we found that the etch rate increases with the concentration of the etchant and the etching temperature. This type of behavior was not observed by Glender and Hauser [30]. In their studies they concluded that the increase in water content (decrease in concentration) increases the etch rate of silicon nitride. But the significant difference to be noted here is that their studies were performed in the temperature range of 140–200 °C, which is close to the boiling point of the phosphoric acid with respective concentrations. They also indi-

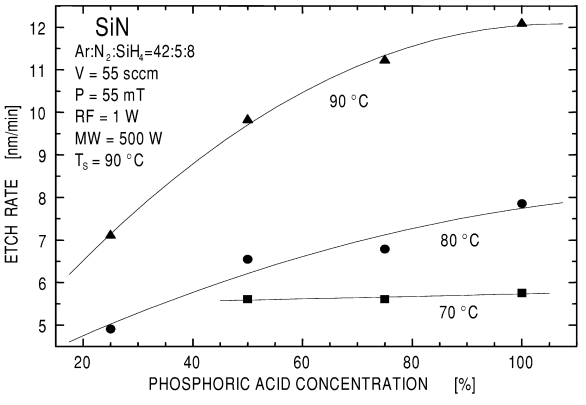

Fig. 5. Variation of etch rate with concentration of phosphoric acid in water for etching temperatures 70, 80, and 90 °C.

cated that the boiling point increases with the concentration. In the present work, the etching was carried out in the temperature range of 70–90 °C, much below the boiling point of the phosphoric acid. Further their films were deposited by using pyrolytic process with SiH_4 and NH_3 at 880 °C where as in the present work the films were obtained through an ECR PECVD process using a gas mixture of Ar:N2:SiH_4, giving a different composition for the deposited SiN films with more hydrogen content. Hence the etching mechanism in both cases could be different leading to different etching results. The higher the etching temperature the stronger is the dependence of the etch rate on concentration. Similar results have been obtained for SiN films deposited from precursors with flow rate ratio given in Fig. 4.

3.3. Etching with BOE solutions

Figs. 6 and 7 show the dependence of the etch rate with BOE solution in water on the deposition parameters *P* and flow rate ratio N_2:SiH_4, respectively, for different concentrations of the BOE solution in water. It is found that the etching rate increases with increase in BOE concentration. Similar results were observed by Deckert [31] using HF/glycerol mixtures. Etching mechanism of SiN in HF based solutions obeys the overall reactions as described by other authors [25,32]:

$$Si_3N_4 + 18HF = H_2SiF_6 + 2(NH_4)_2SiF_6 \qquad (2)$$

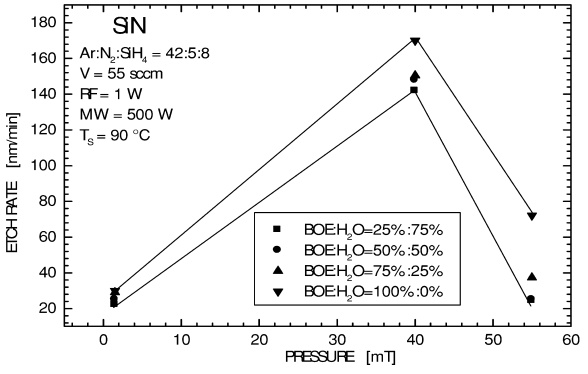

Fig. 6. Dependence of etch rate at 25 °C on deposition pressure for BOE solutions in water as given in figure. Lines are drawn only to guide eyes.

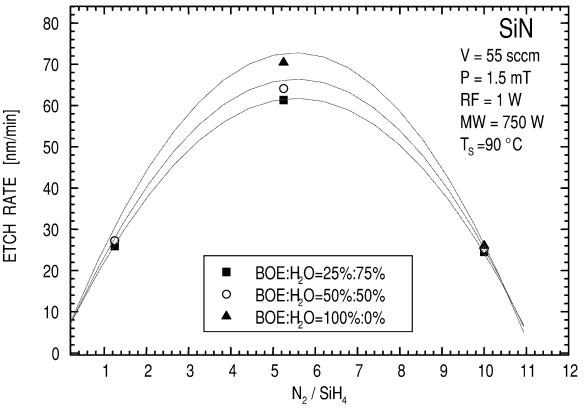

Fig. 7. Etch rate at 25 °C as a function of gas flow rate ratio of precursors for different concentrations of BOE solution in water.

BOE etch rate depends strongly on the deposition pressure (Fig. 6). The dependence is not linear. It passes through a maximum. For the given combination of deposition parameters given in the figure, the SiN films deposited at either very low pressure (~1.5 mT) or very high pressure (~55 mT) have the lowest etch rate. The gas flow rate ratio, N_2:SiH_4, has a strong influence (Fig. 7) on etching with BOE solution. As in the previous case the dependence passes through a maximum. Compared to the etching with phosphoric acid the etch rate with BOE solution is very high. For the combination of parameters given in the figure the lowest etch rate is 20 nm/min either for very low N_2:SiH_4 (~0.62) or very high N_2:SiH_4 (~10). For N_2:SiH_4 = ~5.5 the etch rate is the highest (60 nm/min), which is just the reverse of the etching with phosphoric acid. These results indicate that the etching mechanism with BOE solution is different from that with phosphoric acid.

4. Conclusions

Wet etching studies using phosphoric acid and BOE solutions have been performed on high-density plasma (ECR-PECVD) deposited SiN films. The SiN films were deposited by varying the parameters of deposition namely the pressure, power and the flow ratio of the precursor gases. The etch rate with BOE is much higher than that with phosphoric acid. For both cases, however, the etch rate depends strongly

on deposition pressure and gas flow rate ratio of precursors. The dependence passes through a minimum for etching with phosphoric acid but through a maximum for etching with BOE solution. These results indicate a different mechanism of etching in each case. The stoichiometry of silicon, nitrogen and hydrogen in the film plays a crucial role in the wet etching mechanism of SiN film using phosphoric acid and BOE solutions.

References

[1] Y. Tsividis, Operation and Modeling of the MOS Transistor, 2nd Edition, McGraw-Hill, Boston, 1999.
[2] Y. Manabe, T. Mitsuyu, J. Appl. Phys. 66 (1989) 2475.
[3] R. German, H.W.M. Saleminik, R. Beyeler, G.L. Bona, F. Horst, I. Massarek, B.J. Offrein, Electrochem. Soc. Proc. 99–6 (1999) 169.
[4] K.B. Sundaram, S.S. Seshan, Electrochem. Soc. Proc. 97–6 (1997) 143.
[5] W. Ting, J. Ahn, D.L. Kwong, J.Y.C. Sun, M. Arienzo, IEEE Trans. Electron. Devices ED–37 (1990) 177.
[6] J. Wang, D.A. Thomson, J.G. Simmons, M. Boumerzong, M. Boudreau, P. Mascher, J. Electrochem. Soc. 142 (1995) 593.
[7] G.J. Valco, V.J. Kapoor, M.D. Biendenbender, W.D. Williams, J. Electrochem. Soc. 136 (1989) 175.
[8] G.T.A. Kovacs, Micromachined Transducers Sourcebook, McGraw-Hill, Boston, 1998.
[9] M. Madou, Fundamentals of Microfabrication, CRC Press, New York, 1997.
[10] R.C. Jaegrer, Introduction to Microelectronics Fabrication, Prentice-Hall, Englewood Cliffs, NJ, 1998, pp. 170.
[11] S. Matsuo, K. Kikuchi, Jpn. J. Appl. Phys. 66 (1980) L210.
[12] R.E. Sah, U. Weimar, H. Baumann, J. Wagner, R. Kiefer, S. Müller, Electrochem. Soc. Proc. 97 (1997) 178.
[13] J.C. Barbour, H.J. Stein, O.A. Popov, M. Yoder, C.A. Outten, J. Vac. Sci. Technol. A 9 (1991) 480.
[14] J. Yota, M. Janani, L.E. Camilletti, A. Kar-Roy, Q.Z. Liu, C. Nguyen, M.D. Woo, J. Hander, P. van-Cleemput, IEEE (2000), 0-7803-6327-2/00.
[15] S. Okuda, Y. Shioya, H. Kashimada, J. Electrochem. Soc. 145 (1998) 1338.
[16] J.L. Vossen, W. Kern, Thin Film Processes II, Academic Press, Boston, 1991, pp. 671–748.
[17] Y. Katoka, S. Saito, K. Omiya, J. Electrochem. Soc. 146 (1999) 3435.
[18] R.J. Olson Jr., T.E. Kazior, B. Lane, W.M. Holber, L. Bourget, J. Electrochem. Soc. 143 (1996) 288.
[19] K.R. Williams, R.S. Muller, J. Microelectromech. Syst. 5 (4) (1996).
[20] G. Beshkov, V. Lazarova, D.B. Dimitrov, J. Non-Cryst. Solids 187 (1995) 301.
[21] Y.M. Efimov, Z.V. Panova, A.V. Malygyn, A.P. Kovchartsev, Phys. Status Solidi A 129 (1992) 483.
[22] L.M. Loewenstein, C.M. Tupton, J. Electrochem. Soc. 138 (1991) 1389.
[23] J.D. Plummer, M.D. Deal, P.B. Griffin, Silicon VLSI Technology Fundamentals, Practice and Modeling, Prentice-Hall, Englewood Cliffs, NJ, 2000, pp. 618.
[24] L. Zambov, G. Peev, V. Shanov, S. Drumeva, Vacuum 43 (1992) 227–230.
[25] D.M. Knotter, T.J.J. Denteneer, J. Electrochem. Soc. 148 (2001) F43–F46.
[26] K.A. Buckle, J. Rodgers, K. Pastor, C. Constantine, D. Johnson, Appl. Phys. Lett. 60 (1992) 2601.
[27] W.A. Lanford, Nucl. Instrum. Methods 149 (1978) 1.
[28] W.K. Chu, J.W. Mayer, M.A. Nicolet, Backscattering Spectrometry, Academic Press, New York, 1978.
[29] D.F. Herring, Phys. Rev. 112 (1958) 1217.
[30] W. van Gelder, V.E. Hauser, J. Electrochem. Soc. 114 (1967) 869–872.
[31] C.A. Deckert, J. Electrochem. Soc. 127 (1980) 2433–2438.
[32] L. Zambov, G. Peev, V. Shanov, S. Drumeva, Vacuum 43 (1992) 227–230.